Video Article

Rigid Embedding of Fixed and Stained, Whole, Millimeter-Scale Specimens for Section-free 3D Histology by Micro-Computed Tomography

Alex Y. Lin[1,2], Yifu Ding[1,2,3], Daniel J. Vanselow[1,2], Spencer R. Katz[1,2,3], Maksim A. Yakovlev[1,2], Darin P. Clark[4], David Mandrell[5], Jean E. Copper[1,2], Damian B. van Rossum[1,2], Keith C. Cheng[1,2]

[1]The Jake Gittlen Laboratories for Cancer Research, Penn State College of Medicine

[2]Division of Experimental Pathology, Department of Pathology, Penn State College of Medicine

[3]Medical Scientist Training Program, Penn State College of Medicine

[4]Center for In Vivo Microscopy, Duke University Medical Center

[5]KTM Research

Correspondence to: Keith C. Cheng at kcc2@psu.edu

URL: https://www.jove.com/video/58293
DOI: doi:10.3791/58293

Keywords: Bioengineering, Issue 140, X-ray micro-computed tomography, micro-CT acrylic resin, embedding, model organisms, zebrafish, millimeter-scale, three-dimensional imaging, tissue architecture, complete morphological phenotyping, phenomics

Date Published: 10/17/2018

Citation: Lin, A.Y., Ding, Y., Vanselow, D.J., Katz, S.R., Yakovlev, M.A., Clark, D.P., Mandrell, D., Copper, J.E., van Rossum, D.B., Cheng, K.C. Rigid Embedding of Fixed and Stained, Whole, Millimeter-Scale Specimens for Section-free 3D Histology by Micro-Computed Tomography. *J. Vis. Exp.* (140), e58293, doi:10.3791/58293 (2018).

Abstract

For over a hundred years, the histological study of tissues has been the gold standard for medical diagnosis because histology allows all cell types in every tissue to be identified and characterized. Our laboratory is actively working to make technological advances in X-ray micro-computed tomography (micro-CT) that will bring the diagnostic power of histology to the study of full tissue volumes at cellular resolution (*i.e.*, an X-ray Histo-tomography modality). Toward this end, we have made targeted improvements to the sample preparation pipeline. One key optimization, and the focus of the present work, is a straightforward method for rigid embedding of fixed and stained millimeter-scale samples. Many of the published methods for sample immobilization and correlative micro-CT imaging rely on placing the samples in paraffin wax, agarose, or liquids such as alcohol. Our approach extends this work with custom procedures and the design of a 3-dimensional printable apparatus to embed the samples in an acrylic resin directly into polyimide tubing, which is relatively transparent to X-rays. Herein, sample preparation procedures are described for the samples from 0.5 to 10 mm in diameter, which would be suitable for whole zebrafish larvae and juveniles, or other animals and tissue samples of similar dimensions. As proof of concept, we have embedded the specimens from *Danio*, *Drosophila*, *Daphnia*, and a mouse embryo; representative images from 3-dimensional scans for three of these samples are shown. Importantly, our methodology leads to multiple benefits including rigid immobilization, long-term preservation of laboriously-created resources, and the ability to re-interrogate samples.

Video Link

The video component of this article can be found at https://www.jove.com/video/58293/

Introduction

Phenotypes are observable traits of an organism that represent the consequences of unique interactions between its genetic background and the environment. These characteristics can include behavioral, biochemical, morphological, developmental, and/or physiological properties. Importantly, differences in traits between wild-type organisms and genetic mutants can provide key insight into the mechanisms and functions of affected genes. With respect to morphology, histopathology is the gold standard for assessing phenotypes at the cellular level but suffers from mechanical artifacts and does not allow accurate quantitative volumetric analysis[1]. Our laboratory is motivated to overcome the barriers to the application of the diagnostic power of histology to full tissue volumes at submicron resolution.

A survey of available technologies suggests that imaging by X-ray micro-computed tomography (micro-CT) may provide ideal capabilities needed for millimeter-scale whole-animal 3-dimensional (3D) histology. Micro-CT enables non-destructive, isotropic, 3D visualization and the ability to conduct quantitative analysis of tissue architecture[1,2]. In recent years, 3D imaging of unstained and metal-stained zebrafish by micro-CT has gained increasing traction and has been utilized for volumetric analysis of several tissues, including muscle, teeth, bone, and adipose tissues[3,4,5,6,7,8,9,10]. Other model organisms and tissue specimens are also amenable to micro-CT imaging. For instance, a pipeline has been introduced for quantifying dense mesoscale neuroanatomy of mouse brains imaged via synchrotron micro-CT[11]. Similarly, an eosin-based staining protocol has been shown to be suitable for soft tissue micro-CT imaging of whole mouse organs[12]. Morphometric analysis of unstained human L3 vertebrae and the visualization of silver-stained human lungs using micro-CT have demonstrated the utility of this technology for human samples[13,14].

Copyright © 2018 Creative Commons Attribution-NonCommercial-NoDerivs 3.0 Unported License

In order to actualize the great promise of micro-CT for complete morphological phenotyping of intact small animals and tissue specimens, a number of hurdles need to be overcome in relation to throughput, resolution, field-of-view, comprehensive cell staining, and long-term preservation. While each of these aspects is critically important, the focus of the present manuscript is the optimization of embedding procedures, with additional notes on sample fixation and staining. Heavy metal staining is useful because the inherent contrast between different soft tissues in micro-CT images is low. The potency of various metal stains, such as osmium tetroxide, iodine, phosphotungstic acid (PTA), and gallocyanin-chromalum, to enhance contrast for micro-CT imaging has been studied[15,16,17]. Uranyl acetate has also been used as a contrasting agent for micro-CT imaging of bone and cartilage[18,19]. PTA as used in our protocol leads to consistent staining of nearly all tissues and cells in whole zebrafish specimens, yielding images that are potentially compatible with histology-like studies through full volumes of tissue.

During micro-CT image acquisition, a 2-dimensional (2D) projection is taken as the sample is rotated by a fraction of a degree and repeated until the sample has completed a 180° or 360° rotation, generating a series of thousands of 2D projections used for the reconstruction of the 3D volume[20]. In this process, any perturbation of the specimen will cause the corresponding 2D projections to be out of alignment, resulting in poorly reconstructed 3D volumes. Sample immobilization is a way to correct for this issue and some current strategies involve submerging the sample in alcohol or embedding in agarose in polypropylene tubes or micropipette tips[3,5,15,16,21,22]. Liquid immersion methods are not ideal because sample movement during image acquisition can occur between imaging sets, resulting in shifted reconstructions of 3D volumes[23]. Further, it is well known that the physical stability of liquid-stored tissue samples is poor in time scales of months to years, as a result of chemical instability and surface abrasion associated with movement of contact points between sample and the container wall (personal observations with fixed animal and human tissue samples).

To reduce the potential for sample movement during imaging, samples can be embedded in agarose[24,25,26], but this practice is associated with the risk of the stain diffusing into agarose thus reducing image contrast[26]. Furthermore, liquid or agarose preparations are prone to physical damage and degrade over time, making them unsuitable for long-term sample storage. We reasoned that a potentially successful and straightforward sample immobilization method could be adapted from that used for electron microscopy specimens. Polymerized resins such as EPON 812 (discontinued and replaced by EMbed 812) are commonly used to provide the hardness required to generate ultrathin sections for electron microscopy[27,28]. Indeed, several comparative studies between X-ray imaging and electron microscopy have demonstrated that the samples embedded in resin can be imaged by X-ray microscopy[29,30]. However, some of the standard practices of electron microscopy do not translate directly to micro-CT imaging. For example, micro-CT imaging of samples with squared resin edges of typical resin blocks and samples cut from those blocks is associated with edge diffraction artifacts that can interfere with imaging. Smoothing resin edges, while possible, is laborious and time-consuming.

While a variety of plastic embedding resins are employed in electron microscopy, the high background associated with harder resins such as Embed 812 led us to test others. We chose LR White due to its low viscosity, low shrinkage, low tendency to form bubbles during polymerization, and lower background. To create edge-free samples, and to minimize the quantity of resin surrounding the sample, we developed the protocols to draw specimens in liquid resin into polyimide tubing prior to the polymerization. Polyimide was chosen for its high thermal stability and high X-ray transmittance so that the removal of the tubing is not necessary for imaging. Finally, we designed a custom micropipette adapter for our sample embedding technique in order to reliably hold the tubing and prevent the contamination of micropipettes. The adapter can be 3D printed from a CAD image file. Taken together, the goal of the sample preparation methods presented here is to make embedding of small samples more straightforward, achieve enhanced staining contrast, rigid immobilization, and long-term storage of intact millimeter-scale specimens.

Protocol

All procedures on live animals were approved by the Institutional Animal Care and Use Committee (IACUC) at the Pennsylvania State University.

1. Day 1: Fixation

1. To improve the fixation and reduce the volume of gut contents, starve the juvenile fish for at least 24 h for a 10 mm specimen, or longer for larger specimens (*e.g.*, 72 h for a 14 mm specimen).
2. Pre-chill 10% Neutral Buffered Formalin (NBF) and 2x Tricaine-S (MS-222, 400 mg/L) on ice to 4 °C.
3. Double the fish water volume with chilled 2x MS-222 for rapid and humane euthanasia.
4. Wait for 30 s (larvae) to 60 s (juveniles) after the fish stops moving.
5. Immerse the fish in chilled 10% NBF for 10 min.
6. Fix the fish in chilled 10% NBF solution overnight in flat-bottomed containers at room temperature.
   NOTE: Flat-bottomed containers are required to minimize the bending of the specimen. The volume of fixative and solutions of all subsequent steps should be at least 20 times the sample volume unless otherwise specified. For 1-5 larval zebrafish, the recommended solution volume is at least 1 mL. Insufficient fixative results in poor fixation, and a surplus of reagent volume does not negatively impact the outcome of the described procedure. For complete fixation of larger fish, slit the belly starting slightly anterior to the anal pore. Use minimal penetration of scissors or knife and apply gentle force away from the fish while cutting to minimize damage to internal organs. Fixation protocols have been described by others[31,32,33].

2. Day 2: Dehydration & Staining

1. Rinse fixed specimens 3 times in 1x phosphate buffered saline (PBS) pH 7.4 for 10 min.
2. Submerge the samples in 35% ethyl alcohol (EtOH) for 20 min at room temperature with gentle agitation.
   NOTE: For all gentle agitation steps, use a tabletop shaker and set for a mixing effect while carefully avoiding bumping and rubbing of the sample against the container surfaces.
3. Submerge the samples in 50% EtOH for 20 min at room temperature with gentle agitation.
4. Dissolve phosphotungstic acid (PTA) powder in water to prepare a 1% w/v stock solution.
5. Dilute the 1% PTA stock solution 3:7 in 100% EtOH to obtain a 0.3% PTA staining solution.

Copyright © 2018 Creative Commons Attribution-NonCommercial-NoDerivs 3.0 Unported License

6. Stain the samples overnight in the 0.3% PTA solution at room temperature with gentle agitation.

3. Day 3: Infiltration

1. Prepare 1:1 v/v mixture of 100% EtOH and LR White acrylic resin and set aside.
2. Rinse 3 times in 70% EtOH for 10 min.
3. Submerge the samples in 90% EtOH for 30 min at room temperature with gentle agitation.
4. Submerge the samples in 95% EtOH for 30 min at room temperature with gentle agitation.
5. Submerge the samples twice in 100% EtOH for 30 min at room temperature with gentle agitation.
6. Submerge the samples in the 1:1 EtOH and LR White acrylic resin mixture overnight at room temperature with gentle agitation.

4. Day 4: Embedding

1. Submerge the samples in 100% LR White resin for 2 h at room temperature with gentle agitation.
2. Replace the resin in step 4.1 with fresh 100% LR White resin and incubate for 1 h at room temperature with gentle agitation.
3. Assemble the embedding apparatus (**Figure 1**).
4. Cut polyimide tubing of appropriate diameter and length.
   NOTE: The tubing with an inner diameter that is at least 0.1 mm larger than the diameter of the specimen is recommended. For typical specimens, a standard length of 30 mm of tubing is used for each sample. When desired, elongated specimens can be accommodated by using longer tubing.
   1. Attach a P1000 micropipette to the wide end of the embedding adapter and insert the polyimide tubing to the narrow end (**Figure 1C**). If the embedding adapter is not available, go to Step 4.3.3. Otherwise, continue to Step 4.4.
   2. Clip off the end of a micropipette tip straight across such that the polyimide tubing fits snugly. Cut at 44 mm from the wide end of a 200 µL yellow micropipette tip for the 0.0403" tubing and 59 mm from bottom of 1 mL blue tip for the 0.105" tubing. Trim as needed.
   3. Attach the cut micropipette tip to a micropipette.
5. Transfer the samples to a small weigh boat or V-shaped solution basin and fully submerge the samples in 100% LR White resin.
6. With the embedding apparatus from Step 4.3, aim the tubing at the wide end of the fixed sample (or towards the head in the case of animal specimens) and pipette the specimen slowly into the tubing. Position the sample in the middle of the tubing and ensure the tubing above and below the specimen is filled with resin.
   1. Pipette the sample into the tubing such that the sample is moving in the natural, forward direction.
      NOTE: Slow pipetting avoids air bubbles and specimen damage caused by abrasion against the tubing edge. Backward movement into the tubing can easily damage extremities (limbs, wings, fins, *etc.*). It is recommended to allow some resin overflow in the embedding apparatus so that, later, air does not enter the tubing during removal.
7. Immediately seal the open end with oil-based soft modeling clay.
   1. Flatten the clay into a 1 mm-thick sheet.
   2. Stabilize the tubing between index and middle fingers.
   3. Slowly press the clay against the end of the tubing with thumb.
   4. Remove excess clay.
8. Remove the embedding apparatus from the micropipette.
9. Pull out the tubing by gentle rotation and seal the other end with the clay.
   1. Hold a finger against the sealed end to prevent the ejection of the clay.
   2. Slowly push the unsealed end of the tubing into the clay.
10. Place the tubing horizontally and polymerize the resin for 24 h at 65 °C.
    NOTE: Horizontal placement avoids the sample movement during polymerization. If a small amount of air was trapped in Step 4.8, the end with the air bubble may be elevated slightly to prevent air bubble movement toward the specimen. Importantly, too much elevation during polymerization may cause the specimen to fall towards the low end due to gravity. A properly embedded sample is shown compared to one with an air bubble, which should be avoided because the refraction from air/resin interfaces can degrade image quality (**Figure 2**).

5. Day 5: Collection

1. Collect the samples for image acquisition at the end of Day 5.
   NOTE: The removal of polyimide tubing is possible but not necessary for imaging. Synchrotron-based micro-CT imaging for the zebrafish sample was performed at Beamline 2-BM at Advanced Photon Source (APS) in Argonne National Laboratory (Lemont, IL, USA). For PTA-stained zebrafish, an optimal X-ray energy range of 5-30 keV was determined, and an X-ray energy of 13.8 keV was used for imaging. 1501 projections were obtained at 13.8 keV over 180 degrees (1 projection every 0.12 degrees) with a 2048-by-2048 pixel camera. Additionally, two flat-field (gain) images (one at the beginning and one at the end of the acquisition) and one dark-field image were also acquired. Flat-field and dark-field corrections, ring artifact reduction, and image reconstruction were done using the open source TomoPy toolkit[34]. PTA-stained *Daphnia* and *Drosophila* samples were imaged on an X-ray microscope[12,35]. Specific micro-CT settings are dependent on the object and the quality of the stain. For example, the *Drosophila* specimen was scanned at 40 kVp, 74 mA, and 15 s at a voxel resolution of 3.10 × 3.10 × 3.10 μm^3.

Copyright © 2018 Creative Commons Attribution-NonCommercial-NoDerivs 3.0 Unported License

Representative Results

The protocol described above details the sample preparation procedure for whole zebrafish larvae and juveniles for micro-CT imaging. Notably, this method is readily adapted to other samples types (*e.g.*, *Drosophila*, *Daphnia*, *Arabidopsis*, mouse organs). Incubation times in various steps are appropriate for zebrafish larvae and samples of similar size; larger samples may require longer incubation. To assist with the sample embedding steps, we designed an adapter that attaches to a 1 mL micropipette, and can be customized for various sizes of polyimide tubing (**Figure 1**). This custom adapter was 3D printed from a CAD file that is associated with this manuscript and available for download from http://publications.chenglab.com/LinEtAlJOVE/. Since all readers may not have access to a 3D printer, assembly of a homemade embedding apparatus using micropipette tips is described in the protocol (Step 4.3). A successfully embedded zebrafish larva is shown compared to a specimen with an air bubble (**Figure 2**), which will likely degrade the image quality. To demonstrate the versatility of the embedding procedure, we show the specimens from various model organisms (*i.e.*, *Danio*, *Drosophila*, *Daphnia*, mouse embryo) that have gone through the sample preparation pipeline (**Figure 3**). Reconstructed 3D volumes of whole *Danio*, *Daphnia*, and *Drosophila* specimens imaged by micro-CT are shown (**Figure 4**). Importantly, as demonstrated by the *Danio* sample, these specimens can be stored for an extended period of time and reused for multiple imaging sessions (**Figure 5**).

Copyright © 2018 Creative Commons Attribution-NonCommercial-NoDerivs 3.0 Unported License

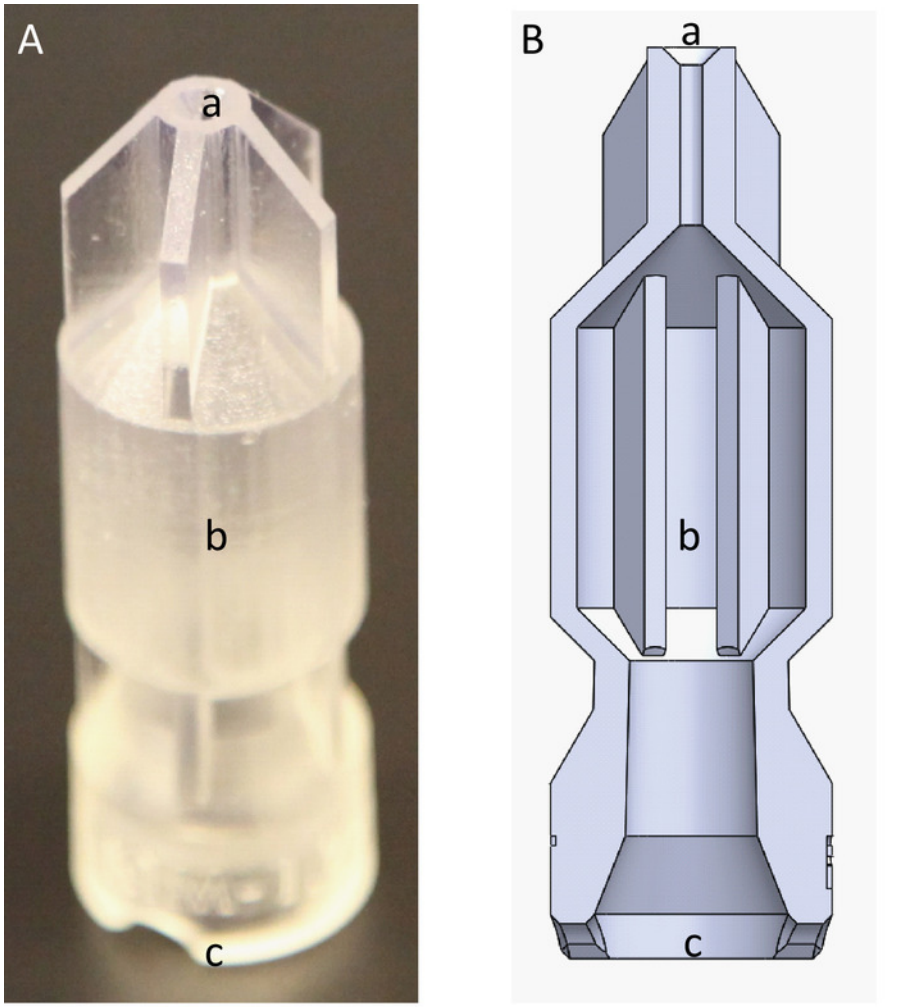

Figure 1. Embedding apparatus. (A) An adapter was designed to facilitate the embedding using common laboratory tools. (B) A cross-sectional illustration of the adapter. (C) The embedding apparatus after the insertion of the polyimide tubing at adapter point (a) and attaching the micropipette at adapter point (c). Adapter segment (b) is an overflow chamber designed to accommodate excess resin and protect the micropipette from contamination. Please click here to view a larger version of this figure.

Copyright © 2018 Creative Commons Attribution-NonCommercial-NoDerivs 3.0 Unported License

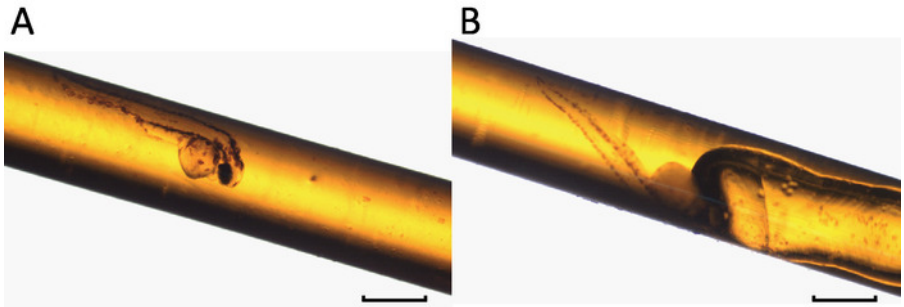

Figure 2. Successfully embedded specimens are devoid of air bubbles. (A) An embedded 3 day post-fertilization (dpf) larval zebrafish without air bubble. (B) An embedded 3 dpf zebrafish with an air bubble. Air trapped during the embedding process can move toward the specimen if the sample is not placed horizontally during the polymerization. Scale bars = 1 mm. Please click here to view a larger version of this figure.

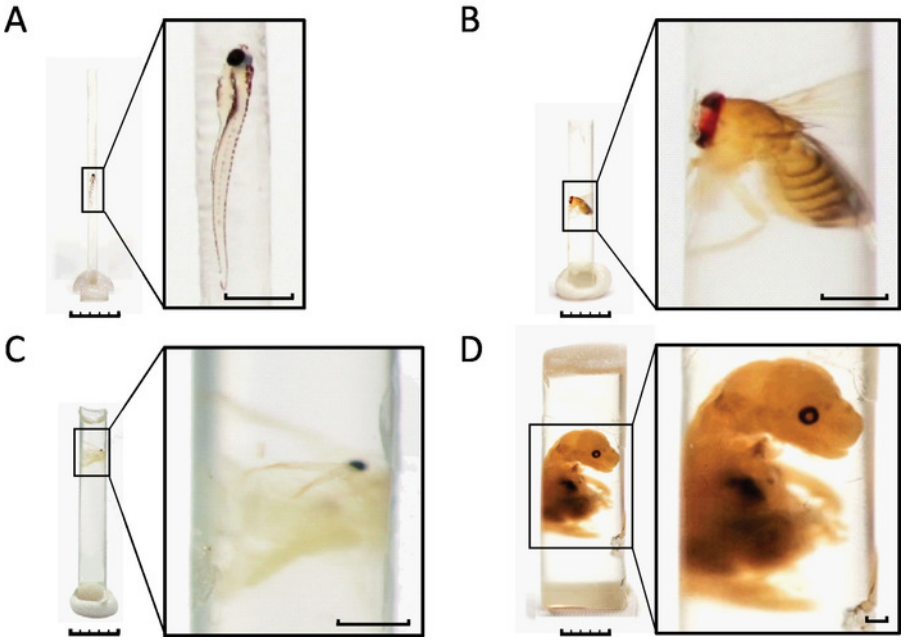

Figure 3. A wide variety of specimens can be embedded with our protocol. (A) 7 dpf zebrafish larva. (B) Adult *Drosophila*. (C) Adult *Daphnia*. (D) Mouse embryo. Larger samples such as the mouse embryo are accommodated by a few modifications to the protocol. Briefly, the polyimide tubing was filled to 1/3 of its length with resin and polymerized prior to embedding. Fixed and stained sample was placed on top of the pre-polymerized resin. The tubing was then filled with un-polymerized resin followed by a second polymerization. The polyimide tubing was removed prior to photography to allow better visualization of the sample in this figure. The removal of the tubing is not necessary for successful image acquisition by micro-CT. Scale bars: specimen images, 5 mm; enlarged insets, 1 mm. Please click here to view a larger version of this figure.

Copyright © 2018 Creative Commons Attribution-NonCommercial-NoDerivs 3.0 Unported License

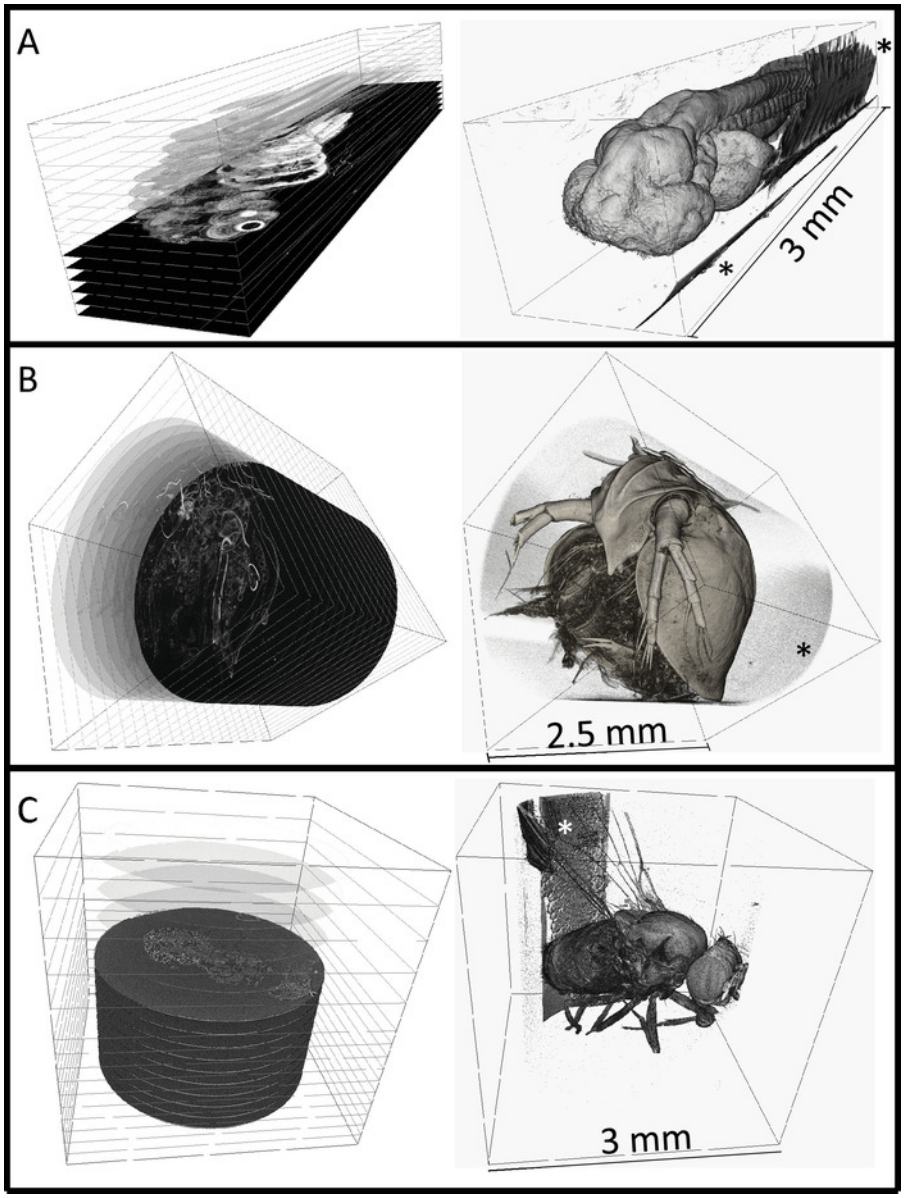

Figure 4. 3-dimensional renderings of embedded specimens. (A) Reconstructed 3 dpf zebrafish larva at 0.743 × 0.743 × 0.743 μm^3 voxel resolution. (B) Reconstructed adult *Daphnia* (3 × 3 × 3 μm^3 voxel resolution). (C) Reconstructed adult *Drosophila* (3.1 × 3.1 × 3.1 μm^3 voxel resolution). Digital cross-sections can be generated at any angle as shown on the left column. Surface renderings are shown on the right, rendered using commercial software. Embedding resin can be seen in all scans outside of the sample (noted by *), but does not interfere with the sample itself. The zebrafish larva was imaged at Argonne National Laboratory at the Advanced Photon Source that is synchrotron-based. The *Daphnia* or *Drosophila* specimens were imaged with a commercial X-ray microscope. Please click here to view a larger version of this figure.

Copyright © 2018 Creative Commons Attribution-NonCommercial-NoDerivs 3.0 Unported License

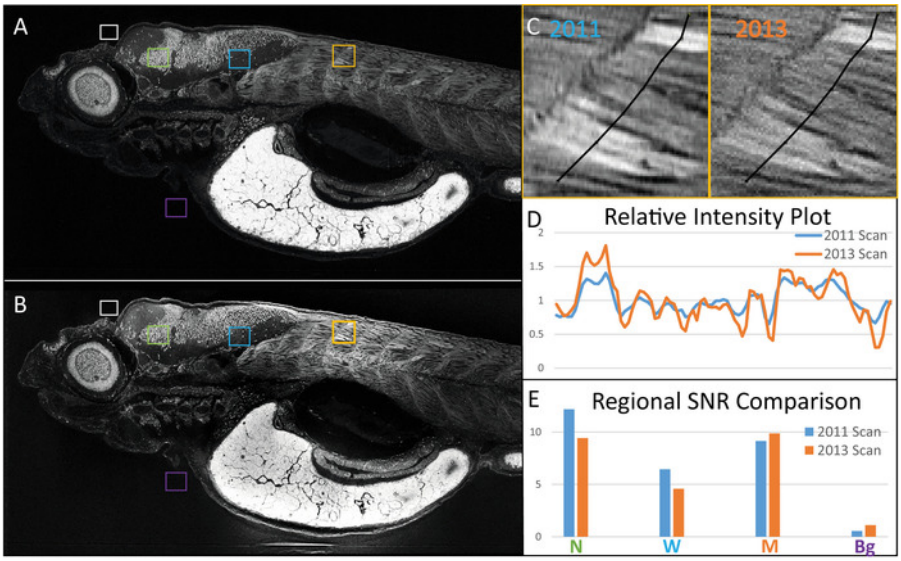

Figure 5. Samples embedded with our protocol can be re-imaged with micro-CT. The same 5 dpf zebrafish larva was imaged in (A) 2011 and (B) 2013, presented as average intensity projections of the sagittal view. Image comparison between scans after the storage shows the preservation of anatomical features. (C) A close-up of muscle from both scans is presented, with segmented lines indicating corresponding regions used for (D) intensity profile generation. Intensity profiles normalized to their corresponding averages along both lines show spatially matching local peaks in both scans. (E) Average intensity values for selected regions in A and B belonging to background (Bg, purple), neuronal nuclei (N, green), white matter (W, blue), and the muscle (M, orange) were divided by an average for background (white) and used to generate signal-to-noise ratios (SNR), which corresponds well between scans. Scale bars = 100 µm. Please click here to view a larger version of this figure.

Discussion

In this manuscript, we present a detailed protocol for rigid immobilization of fixed and stained millimeter-scale (0.5 to 2.5 mm diameter) specimens for micro-CT imaging. Given the rapid advance of micro-CT technology with regard to resolution and speed, a method of permanent sample preservation with re-imaging capabilities is highly desirable. Traditionally, dense embedding resin are commonly used in electron microscopy to provide structural support to cut ultrathin sections and minimize the damage to the specimen. Our method adapted its use for rigid immobilization during non-destructive imaging. To minimize the imaging artifacts from the presence of excess resin, we have implemented the use of X-ray transparent polyimide tubing to create round samples without edges, and to restrict the volume of resin around the sample.

Optimal outcome of the embedding procedure is contingent upon careful execution of several critical steps and attention to sample integrity throughout the procedure. Indeed, damaging the specimen will result in a compromised final image regardless of the success of execution of imaging. Since chilling contributes to a diminution of pain responses, and unfixed tissue degrades more rapidly at higher temperatures, we use pre-chilled reagents. Large specimens may need to be cut to allow the entry of fixative into the inside of the specimen so that internal organs such as liver, pancreas, and gut are completely fixed. Unfixed tissues deteriorate and lose structural integrity, destroying biological structure. Another key step is to maintain the specimen in its natural alignment. Therefore, we advocate for the use of flat-bottomed containers, which we use throughout the procedure and are particularly important during fixation. Fixation in polypropylene tubes or conical tubes that usually have a V-shaped bottom should be avoided because they can cause elongated samples to bend, which distorts the natural morphology of the specimen. In addition, to minimize the use of resin, the inner diameter of the polyimide tubing is only slightly larger than the width of the specimen. Bending of the specimen can also result in damage to the specimen as it enters the tubing. It is also recommended to transfer the specimen into the tubing in a natural forward manner to avoid damaging extremities. Proper dehydration is another critical step. This is accomplished with small increments of increasing EtOH concentrations to slowly replace water with EtOH, which is more miscible with the resin. Large increases in EtOH concentration are associated with tissue shrinkage and can be ameliorated by additional increments of EtOH incubation to make the transition more gradual. Finally, to minimize the movement of the specimen or air pockets, if there are any, the samples are placed horizontally during the resin polymerization (end of Day 4). Air pockets or sealant next to the specimen causes optical artifacts with X-ray imaging associated with edge diffraction, reducing image quality.

With respect to possible modifications to the protocol, other embedding resins and metal stains can be used in place of LR White acrylic and PTA, respectively. Embed812, an epoxy resin commonly used in electron microscopy, is highly viscous, more difficult to transfer, may cause the distortion of the specimens, and is associated with higher background than acrylic or glycol methacrylate resins. While JB4 Plus, a glycol methacrylate, is less viscous than EMbed812 and has lower background, random formation of air pockets frequently appear in the vicinity of the specimen. As mentioned, air pockets degrade the image quality and are particularly problematic for precious samples. It is worth noting that Technovit 7100, another glycol methacrylate, interferes with PTA staining, resulting in poor contrast in the final image. Comparatively, LR White acrylic has water-like viscosity, low background, and does not interfere with PTA staining. In our hands, the success rate of embedding in LR White without sample damage or air bubbles is greater than 95%. For these reasons, we advocate its use as the embedding resin for tissue micro-CT. With respect to stains, the outcome of various metal stains such as osmium tetroxide, iodine, and PTA in micro-CT imaging has been compared and discussed elsewhere[15,16,17] and is outside the scope of this manuscript.

Copyright © 2018 Creative Commons Attribution-NonCommercial-NoDerivs 3.0 Unported License

The sample size is a major limitation to our current protocol. Since we employ suction to transfer specimens into the tubing, the ability to see the specimen is critical for orientation and ensuring that it is indeed in the tubing. As a result, sub-millimeter samples such as *Tardigrade* (*i.e.*, water bears) are extremely difficult to embed because they require the use a microscope to be visualized. Once suction is applied, microscopic specimens are easily lost from the focal plane and become challenging to rediscover, making it difficult to determine if they passed too far through the attached end of the tubing. Larger samples, such as mouse embryos, (3 - 10 mm) can be embedded with slight modifications to the embedding protocol (**Figure 4D**). In particular, the polyimide tubing was filled to 1/3 with liquid resin, which was polymerized prior to embedding. The fixed and stained sample was placed on top of the pre-polymerized resin. The tubing was then fully filled with un-polymerized resin and followed by a second polymerization.

The significance of our embedding protocol is manifold. Rigidly immobilized whole animal or tissue specimens are desirable for reasons including: (1) creating long-term repositories of samples that are difficult to generate or prepare; (2) re-acquisition of data; (3) enabling serial imaging using multiple imaging modalities; and (4) providing standards for calibration and technology development. Samples prepared with our embedding procedure are encased in solid resin that is resilient against damage and can therefore be easily stored perhaps indefinitely. Long-term storage is particularly useful for rare or laboriously generated specimens such as those associated with phenome projects. Further, in the event that the digital data are lost, the data can be generated from the original sample. The capability of re-imaging over a long period of time potentially allows the same sample to be interrogated with more advanced imaging modalities in the future. Since the samples are physically stable between imaging instances, images are acquired from the same specimen in the same orientation, facilitating registration between earlier and later data sets. For example, a low-resolution image may only allow segmentation of tissues in a zebrafish larva. The same larva can later be re-imaged at higher-resolution so that more detailed computational analyses at cellular resolution. This capability for direct comparison between registered scans suggests resin-embedded samples as a potential standard for technology development of micro-CT. The effects of any alteration to the imaging method can be assessed by imaging of the same sample so that all variables in the sample preparation step are controlled. Finally, a resin-embedded standard sample can be used for instrument calibration to test for consistency of imaging.

Our previous work examining mutant and diseased fish histology showed that cellular resolution allows detection of subtle abnormalities in tissue structure that are overlooked in gross examination using the dissecting microscope[36], or a low-power stereo microscope. We wish to expand our high-resolution analyses to human samples. Zebrafish larvae, which comprise the primary subject of our development work, are similar to human needle biopsies in their fragility, cellular and intercellular tissue heterogeneity, size (1-3 mm diameter), and elongated shape. Based on our extensive experience with zebrafish, and other work showing that micro-CT successfully stained and scanned human tissue, albeit at lower resolution[37], we expect our approaches to bring added value to imaging and analysis of needle biopsies. We have estimated that the assembly of a kit sufficient for one preparation of up to 20 samples of the same condition to be potentially less than 30 USD. The samples prepared by our embedding method are resistant to physical damage and therefore easy to transport. The low cost and ease of transport suggest the possibility of collection of samples from across the world, particularly areas in which cellular resolution imaging with micro-CT is not readily accessible. Our vision is for high resolution digital files of needle biopsies (ranging from 0.1 to several terabytes) to enable the creation of a digital atlas of human tissues, and at the same time allow the researchers to refine and enhance current analysis pipelines for localization and quantitative characterization of cellular and tissue architecture within the full 3D context of the tissues scanned.

Disclosures

All of the authors declare that there are no conflicts of interests.

Acknowledgements

The authors would like to thank Roland Myers for kindly providing the original TEM protocols. In addition, we would like to thank Dr. John Colbourne for providing the *Daphnia* specimen, Dr. Santhosh Girirajan for providing the *Drosophila* specimen, and Dr. Fadia Kamal for providing the mouse embryo. The investigators acknowledge funding support from the NIH (1R24OD18559-01-A2, PI: KCC), the Jake Gittlen Laboratories for Cancer Research, and from pilot award funding from the PSU Huck Institutes of the Life Sciences and the Institute for CyberScience.

References

1. Cheng, K.C., Katz, S.R., Lin, A.Y., Xin, X., Ding, Y. Whole-organism cellular pathology: a systems approach to phenomics. *Advances in Genetics.* **95**, 89-115 (2016).
2. Cheng, K.C., Xin, X., Clark, D., La Riviere, P. Whole-animal imaging, gene function, and the zebrafish phenome project. *Current Opinion in Genetics & Development.* **21** (5), 620-629 (2011).
3. Vågberg, W., Larsson, D.H., Li, M., Arner, A., Hertz, H.M. X-ray phase-contrast tomography for high-spatial-resolution zebrafish muscle imaging. *Scientific Reports.* **5**, 16625 (2015).
4. Bruneel, B. *et al.* Imaging the zebrafish dentition: from traditional approaches to emerging technologies. *Zebrafish.* **12** (1), 1-10 (2015).
5. Charles, J.F. *et al.* Utility of quantitative micro-computed tomographic analysis in zebrafish to define gene function during skeletogenesis. *Bone.* **101**, 162-171 (2017).
6. Silvent, J. *et al.* Zebrafish skeleton development: High resolution micro-CT and FIB-SEM block surface serial imaging for phenotype identification. *PLoS One.* **12** (12), e0177731 (2017).
7. Hur, M. *et al.* MicroCT-based phenomics in the zebrafish skeleton reveals virtues of deep phenotyping in a distributed organ system. *eLife.* **6**, e26014 (2017).
8. Seo, E., Lim, J.H., Seo, S.J., Lee. S.J. Whole-body imaging of a hypercholesterolemic female zebrafish by using synchrotron X-ray micro-CT. *Zebrafish.* **12** (1), 11-20 (2015).
9. Hasamura, T. *et al.* Green tea extract suppresses adiposity and affects the expression of lipid metabolism genes in diet-induced obese zebrafish. *Nutrition and Metabolism.* **9** (1), 73 (2012).

Copyright © 2018 Creative Commons Attribution-NonCommercial-NoDerivs 3.0 Unported License

10. Meguro, S., Hasumura, T., Hase, T. Body fat accumulation in zebrafish is induced by a diet rich in fat and reduced by supplementation with green tea extract. *PLoS One.* **10** (3), e0120142 (2015).
11. Dyer, E.L. *et al.* Quantifying mesoscale neuroanatomy using X-ray microtomography. *eNeuro.* **4** (5) (2017).
12. Busse, M. *et al.* Three-dimensional virtual histology enabled through cytoplasm-specific X-ray stain for microscopic and nanoscopic computed tomography. *Proc Natl Acad Sci U.S.A.* **115** (10), 2293-2298 (2018).
13. Perilli, E., Parkinson, I.H., Reynolds, K.J. Micro-CT examination of human bone: from biopsies towards the entire organ. *Ann Inst Super Sanita.* **48** (1), 75-82 (2012).
14. Watz, H., Breithecker, A., Rau, W.S., Kriete, A. Micro-CT of the human lung: imaging of alveoli and virtual endoscopy of an alveolar duct in a normal lung and in a lung with centrilobular emphysema - initial observations. *Radiology.* **236** (3), 1053-1058 (2005).
15. Metscher, B.D. MicroCT for developmental biology: A versatile tool for high-contrast 3D imaging at histological resolutions. *Developmental Dynamics.* **238** (3), 632-640 (2009).
16. Metscher, B.D. MicroCT for comparative morphology: simple staining methods allow high-contrast 3D imaging of diverse non-mineralized animal tissues. *BMC Physiology.* **9**, 11 (2009).
17. Pauwels, E., Van Loo, D., Cornillie, P., Brabant, L., Van Hoorebeke, L. An exploratory study of contrast agents for soft tissue visualization by means of high resolution X-ray computed tomography imaging. *Journal of Microscopy.* **250** (1), 21-31 (2013).
18. Kün-Darbois, J.D., Manero, F., Rony, L., Chappard, D. Contrast enhancement with uranyl acetate allows quantitative analysis of the articular cartilage by microCT: Application to mandibular condyles in the BTX rat model of disuse. *Micro.* **97**, 35-40 (2017).
19. Tang, S.Y., Vashishth, D. A non-invasive *in vitro* technique for the three-dimensional quantification of microdamage in trabecular bone. *Bone.* **40** (5), 1259-1264 (2007).
20. Elliott, J.C., Dover, S.D. X-ray microtomography. *Journal of Microscopy.* **126** (Pt 2), 211-213 (1982).
21. Johnson, J.T. *et al.* Virtual histology of transgenic mouse embryos for high-throughput phenotyping. *PLoS Genetics.* **2** (4), e61 (2006).
22. Larsson, D.H., Vågberg, W., Yaroshenko, A., Yildirim A.Ö., Hertz, H.M. High-resolution short-exposure small-animal laboratory x-ray phase-contrast tomography. *Scientific Reports.* **6**, 39074 (2016).
23. Pleissis, A., Broeckhoven, C., Guelpa, A., Roux, S. G. Laboratory x-ray micro-computed tomography: a user guideline for biological samples. *GigaScience.* **5**, 1011 (2017).
24. Wong, M.D., Spring, S., Henkelman, R.M. Structural stabilization of tissue for embryo phenotyping using micro-CT with iodine staining. *PLoS One.* **8** (12), e84321 (2013).
25. Wong, M.D., Maezawa, Y., Lerch, L.P., Henkelman, R.M. Automated pipeline for anatomical phenotyping of mouse embryos using micro-CT. *Development.* **141** (12), 2533-2541 (2014).
26. Hsu, C.W. *et al.* Three-dimensional microCT imaging of mouse development from early post-implantation to early postnatal stages. *Developmental Biology.* **419** (2), 229-236 (2017).
27. Luft, J.H. Improvements in epoxy resin embedding methods. *The Journal of Biophysical and Biochemical Cytology.* **9**, 409-414 (1961).
28. Hayat, M.A., Giaquinta, R. Rapid fixation and embedding for electron microscopy. *Tissue Cell.* **2** (2), 191-195 (1970).
29. Handschuh S., Baeumler, N., Schwaha, T., Ruthensteiner, B. A correlative approach for combining microCT, light and transmission electron microscopy in a single 3D scenario. *Frontiers in Zoology.* **10**, 44 (2013).
30. Bushong, E. A. *et al.* X-ray microscopy as an approach to increasing accuracy and efficiency of serial block-face imaging for correlated light and electron microscopy of biological specimens. *Microscopy and Microanalysis.* **21** (1), 231-238 (2015).
31. Tsao-Wu, G.S., Weber, C.H., Budgeon, L. R., Cheng, K.C. Agarose-embedded tissue arrays for histologic and genetic analysis. *Biotechniques.* **25** (4), 614-8 (1998).
32. Sabaliauskas, N.A. *et al.* High-throughput zebrafish histology. *Methods.* **39** (3), 246-54 (2006).
33. Copper, J.E. *et al.* Comparative analysis of fixation and embedding techniques for optimized histological preparation of zebrafish. *Comparative Biochemistry and Physiology.* **208**, 38-46 (2018).
34. Merkle, A.P., Gelb, J. The ascent of 3D X-ray microscopy in the laboratory. *Microscopy Today.* **21** (2), 10-15 (2013).
35. Gürsoy, D., De Carlo, F., Xiao, X., Jacobsen, C. TomoPy: a framework for the analysis of synchrotron tomographic data. *J Synchrotron Radiat.* **21** (Pt 5): 1188-93 (2014).
36. Thomas, G.K. *A molecular and systems biology analysis of pleiotropic vertebrate phenotypes (Doctoral dissertation).* Retrieved from the Penn State Electronic Theses and Dissertations Database. (2009).
37. Walton, L.A. *et al.* Morphological characterisation of unstained and intact tissue micro-architecture by X-ray computed micro- and nano-tomography. *Scientific Reports.* **5**, 10074 (2015).

Copyright © 2018 Creative Commons Attribution-NonCommercial-NoDerivs 3.0 Unported License